Materials and Design 132 (2017) 367–374

Contents lists available at ScienceDirect

Materials and Design

journal homepage: www.elsevier.com/locate/matdes

Restrained shrinkage cracking of cementitious composites containing soft PCM inclusions: A paste (matrix) controlled response

Zhenhua Wei [a], Gabriel Falzone [a], Sumanta Das [b], Naman Saklani [c], Yann Le Pape [d], Laurent Pilon [e], Narayanan Neithalath [c], Gaurav Sant [a,f,*]

[a] Laboratory for the Chemistry of Construction Materials (LC^2), Department of Civil and Environmental Engineering, University of California, Los Angeles, CA 90095, United States
[b] Department of Civil and Environmental Engineering, University of Rhode Island, Kingston, RI 02881, United States
[c] School of Sustainable Engineering and the Built Environment, Arizona State University, Tempe, AZ 85287, United States
[d] Oak Ridge National Laboratory, Oak Ridge, TN 37831, United States
[e] Department of Mechanical and Aerospace Engineering, University of California, Los Angeles, CA 90095, United States
[f] California Nanosystems Institute, University of California, Los Angeles, CA 90095, United States

HIGHLIGHTS

- The cracking sensitivity of cementitious composites is controlled by the paste (matrix).
- Soft inclusions reduce composite stiffness and enhance stress relaxation without affecting their tensile capacity.
- Soft inclusions provoke crack blunting and deflection, due to their large stiffness contrast with the paste matrix.
- These combined actions substantially enhance cracking resistance of cementitious composites upon dosage of soft inclusions.

GRAPHICAL ABSTRACT

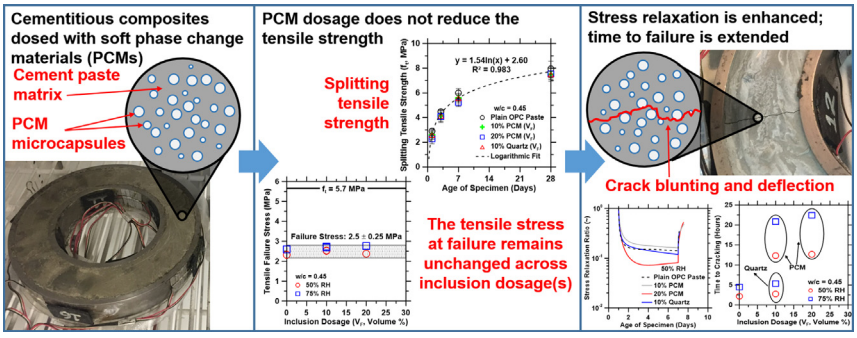

ARTICLE INFO

Article history:
Received 13 February 2017
Received in revised form 28 June 2017
Accepted 29 June 2017
Available online 30 June 2017

Keywords:
Composites
Cracking
Inclusions
Elastic modulus
Strength

ABSTRACT

The addition of phase change materials (PCMs) has been proposed as a means to mitigate thermal cracking in cementitious materials. However, the addition of PCMs, i.e., soft inclusions, degrades the compressive strength of cementitious composites. From a strength-of-materials viewpoint, such reductions in strength are suspected to increase the tendency of cementitious materials containing PCMs to crack under load (e.g., volume instability-induced stresses resulting from thermal and/or hygral deformations). Based on detailed assessments of free and restrained shrinkage, elastic modulus, and tensile strength, this study shows that the addition of PCMs does not alter the cracking sensitivity of the material. In fact, the addition of PCMs (or other soft inclusions) enhances the cracking resistance as compared to a plain cement paste or composites containing equivalent dosages of (stiff) quartz inclusions. This is because composites containing soft inclusions demonstrate benefits resulting from crack blunting and deflection, and improved stress relaxation. As a result, although the tensile stress at failure remains similar, the time to failure (i.e., macroscopic cracking) of PCM-containing composites is considerably extended. More generally, the outcomes indicate that dosages of soft(er) inclusions, and the resulting decrease in compressive strength does not amplify the cracking risk of cementitious composites.

* Corresponding author at: Laboratory for the Chemistry of Construction Materials (LC^2), Department of Civil and Environmental Engineering, University of California, Los Angeles, CA 90095, United States.
E-mail address: gsant@ucla.edu (G. Sant).

http://dx.doi.org/10.1016/j.matdes.2017.06.066
0264-1275/

1. Introduction and background

Microencapsulated phase change materials (PCMs) have been proposed as a means to: (i) reduce the risk of thermal cracking in restrained concretes [1–4], and, (ii) reduce the energy consumption associated with heating and cooling buildings [5–8]. The success of PCMs in these applications is ensured by their ability to absorb heat from their surroundings at temperatures in excess of their phase change temperature (T_{PC}, °C), and release such heat at temperatures below their phase change temperature. Such temperature-dependent absorption and release of heat is often achieved by an organic phase change material ("core"), which for reasons of shape-stabilization, and to ensure its chemical passivity, is enclosed within a polymer encasement ("shell"); e.g., see Fig. 1(a).

Expectedly, on account of their *soft* nature (e.g., typically, the paraffin-based core and polymer shell materials display an elastic modulus on the order of 50 MPa, and 600 MPa, respectively [10–17]) – the dosage of PCMs into cementitious materials has been shown to result in reductions in the compressive strength of the composite [3,10,18] (e.g., see Fig. 1b [10]). If such "strength reductions" are considered in terms of their implications on cracking risk; from a strength of materials perspective (i.e., cracking occurs when the strength of the material is exceeded) – it may be suspected that PCM additions may result in concretes being at a higher risk of cracking. Therefore, despite their advantage of serving as a sink/source for early-age hydration, and environmental heat – the dosage of PCMs into cementitious materials may be counterproductive due to the strength loss, and amplified concrete cracking risk that results.

While a previous study has examined aspects of the durability of mature cementitious composites containing PCMs [9] – but not restrained cracking behavior – to definitively answer the question "Does the addition of microencapsulated PCMs render cementitious materials more sensitive to cracking?" a comprehensive assessment of the mechanical properties and cracking sensitivity is undertaken to contrast the cracking behavior of formulations containing stiff (quartz) inclusions and soft (PCM) inclusions. It is shown that PCM inclusions do not amplify the risk of cracking, but rather, reduce the risk of cracking vis-à-vis stiff inclusion systems. Similar to other soft inclusions (e.g., elastomers, expanded polystyrene, etc. [19–21]), this outcome is attributed to crack blunting and deflection effects, and the improved stress relaxation [10,19–24] resulting from PCM dosage, separate from any heat absorption and release related effects.

2. Materials and experimental methods

An ASTM C150 compliant Type I/II ordinary portland cement (OPC) was mixed with deionized (DI) water to prepare cement pastes and mortars as per ASTM C305 [25]. The OPC used had a nominal composition (in terms of mass %) of: 56.5% C_3S, 18.0% C_2S, 11.4% C_4AF and 6.3% C_3A. An ASTM C778 [26] compliant graded quartz sand was used as stiff inclusions. The soft inclusions comprised a microencapsulated phase change material (MPCM24D, Microtek Laboratories Inc. [27]) which consisted of a paraffinous core encapsulated within a melamine-formaldehyde (MF) shell. The PCM was supplied in the form of a powder, and had a phase change temperature around 24 °C and a latent heat capacity around 162 kJ/kg [5,9,27]. The densities of the OPC, quartz, and microencapsulated PCM were estimated as 3150 kg/m^3, 2650 kg/m^3, and 900 kg/m^3, respectively.

All cementitious mixtures were prepared at a fixed w/c (water-to-cement ratio, mass basis) of w/c = 0.45. The cementitious mixtures formulated consisted of *neat* cement paste, and mortars containing 10 vol% and 20 vol% of quartz or PCM inclusions. Due to their small particle size, it was difficult to formulate *suitably fluid* ("nearly pourable") microencapsulated PCM-containing mixtures at higher inclusion volume fractions without the addition of high-dosages of superplasticizer which substantially alters early-age reaction kinetics. Therefore, higher inclusion dosages were not considered. Herein, each mortar contained only a single type of inclusion (i.e., either quartz sand or microencapsulated PCM), in order to distinguish their influences on restrained cracking behavior. However, in the case of practical concrete proportioning which is carried out on a volumetric basis – the aggregate content is specified as a volume percentage of the overall volume. In circumstances such as these, where the ratio of coarse and fine aggregate in the mixture is defined (fixed), it is expected that PCM inclusions would be dosed by replacing a portion of the fine aggregate by PCM inclusions, volumetrically. Such dosage could be carried out to ensure a particular level of heat absorption and release, or to reduce the cracking risk.

2.1. Particle size distributions

The particle size distributions (PSDs, Fig. 2) of the OPC, quartz, and PCM were measured using Static Light Scattering (SLS) using a Beckman Coulter LS13-320 particle sizing apparatus fitted with a 750 nm light-source. Each solid was dispersed into primary particles via ultrasonication in isopropanol (IPA), which was also used as the carrier

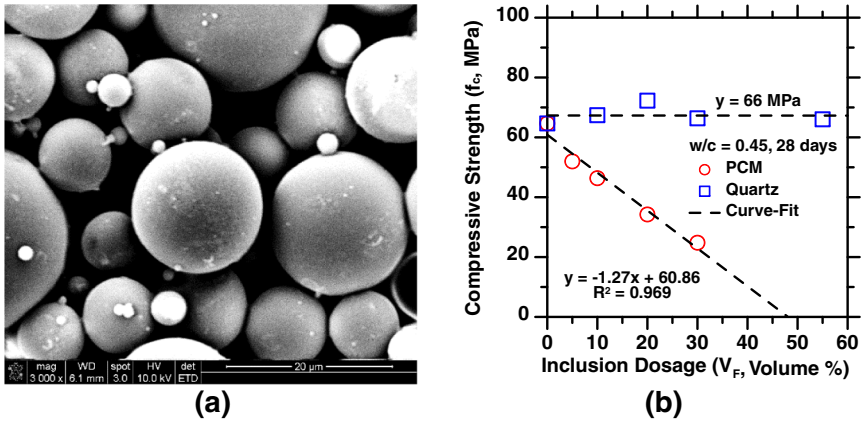

Fig. 1. (a) A scanning electron micrograph of "core-shell" microencapsulated phase change materials (PCMs) wherein the core is the active phase change component (e.g., often alkanes of composition C_nH_{2n+2}) and the shell is a polymer structure often comprised of melamine-formaldehyde (MF) (N.B.: Only the MF shell is visible in this image. For a typical PCM microcapsule (median diameter ≈ 20 μm; see the figure), the shell makes up 5-to-10 vol%, with the remaining fraction occupied by the core. Based on estimates from the series and parallel models for composite stiffness, for the volume fraction bounds noted above the elastic modulus of the core-shell composite (E_{CS}) is estimated to range between 55 MPa ≤ E_{CS} ≤ 200 MPa. Although this example assumes that the core material fully occupies the internal shell volume, in general, PCM particulates show an elastic modulus that is > 100 times smaller than a typical cement paste (see Fig. 3c) – thereby classifying such particles as a "soft inclusion" vis-à-vis the cement paste matrix. [9], and, (b) The compressive strength, f_c, of cementitious mixtures containing quartz or microencapsulated PCM inclusions after 28 days of aging as a function of the inclusion volume fraction (V_F) [10].

fluid. The complex refractive indices of the OPC, quartz, and PCMs were taken as $1.70 + 0.10i$ [28], $1.53 + 0.00i$ [29], and $1.54 + 0.00i$ [30], respectively. The maximum uncertainty in the PSDs was around 6% based on six replicate measurements.

2.2. Splitting tensile strength

The splitting tensile strength (f_t, MPa) of all specimens was measured as per ASTM C496 [31]. The strength measurements were carried out after 1, 3, 7, and 28 days of curing for cylindrical specimens (diameter × height: 101.6 mm × 203.2 mm) maintained at 25 ± 3 °C in saturated limewater. A compressive force was applied along the length of the cylindrical specimen at a rate of 10 kN/s until failure occurred. A thin plywood strip was used to uniformly distribute the load along the length of the cylinder and the maximum load (F_t) borne by the specimen was used to obtain the splitting tensile strength. The tensile strength represents the average of three specimens cast from the same mixing batch.

2.3. Static (compressive) elastic modulus

The elastic (or Young's) modulus (E_C, GPa; N.B.: this represents the chord modulus of elasticity [32]) of all specimens was measured as per ASTM C469 [33]. The elastic modulus measurements were carried out after 1, 3, 7, and 28 days of curing for cylindrical specimens (diameter × height: 101.2 mm × 203.2 mm) maintained at 25 ± 3 °C in saturated limewater using a MTS 311.31 closed-loop servo-hydraulic instrument. A quick-setting gypsum plaster "Hydrostone" was used for capping the specimens to ensure uniform compression at the ends of each cylinder. The reported elastic modulus represents the average of three specimens cast from the same mixing batch.

2.4. Unrestrained shrinkage

Unrestrained deformations of cementitious specimens were measured as described in ASTM C157 [34]. Free shrinkage (ε_{FS}) was measured using prismatic specimens (25.4 mm × 25.4 mm × 285 mm). After saturated curing for the first 24 h, the prismatic specimens were demolded, double-bagged in Ziploc© bags - to ensure partially sealed conditions, and limit water loss - and then stored in an environmental chamber (Darwin KB024) at 25 ± 0.1 °C and 87 ± 0.1% RH for an additional 6 days. The condition of partial sealing was implemented to mimic conditions of the restrained ring setup – which could only be sealed by "double bagging" (see below). After 6 additional days of "partially sealed" (i.e., since the double bagging did not allow perfect sealing) curing, the samples were properly sealed on 4 sides using two-layers of aluminum tape such that only two (long) parallel faces remained unsealed to ensure symmetric (1D) drying – analogous to the conditions of the restrained ring setup. After this time, the samples were stored at 50 ± 0.1% RH and 75 ± 0.1% RH (relative humidity) for an additional three days. Shrinkage and mass loss were measured after 1, 3, 5, 7, 8, 9, and 10 days from the time of casting. The shrinkage and mass loss data shown represent the average of four specimens cast from the same mixing batch. The unrestrained shrinkage thus measured enabled calculation of the elastic stress that would develop – following Hooke's Law – which upon comparison with the measured residual stress allows quantification of the extent of stress relaxation (see below) [35–38].

2.5. Restrained shrinkage

The dual ring test was used to assess the cracking tendency of the cementitious mixtures [3,35–38]. The apparatus consists of two rings (i.e., an inner ring and an outer ring) made of Invar 36 to minimize the influence of temperature on the results. The coefficient of thermal expansion of the Invar 36 is around 2.5 με/°C [3]. The inner Invar ring had an outer radius $R_{I,o}$ of 50.8 mm and an inner radius $R_{I,i}$ of 44.5 mm. The inner ring was instrumented with four strain gauges (CEA-00-350Ω; ε_I) placed at 90° from each other at the mid-height on the inner circumference. The outer invar ring had an outer radius $R_{O,o}$ of 82.6 mm and an inner radius $R_{O,i}$ of 76.2 mm. The outer ring was also instrumented with four strain gauges (CEA-00-350Ω; ε_O) placed at 90° from each another at the mid-height on the outer circumference. Both the inner and outer rings had a height of 25.4 mm. Strains were measured at 5 min intervals, starting about 30 min after mixing until the test was terminated. The instrumented rings were placed at the center of an acrylic base that was coated with a form release agent to minimize bonding. The rings were also coated with a form release agent to prevent restraint due to bonding with the cementitious mixtures. The elastic modulus and Poisson's ratio of the Invar rings were taken as $E_{inv} = 141$ GPa, and $\nu_{inv} = 0.28$, respectively [3].

The fresh cementitious mixture was cast between the two rings and vibrated to ensure consistent filling. The setup was double-bagged in Ziploc© bags and then maintained in a programmable environmental chamber (Darwin KB024) at 25 ± 0.1 °C and 87 ± 0.1% RH to limit moisture loss over the first 7 days. A PVC coversheet formed as an annulus was additionally used to seal the top-surface of the rings to minimize the potential for drying. After 7 days of "partially sealed" curing, the rings were placed on an elevated wire-mesh platform with their top and bottom surfaces exposed, and dried symmetrically at 50 ± 0.1% RH or 75 ± 0.1% RH until cracking occurred. Restrained shrinkage was monitored on duplicate ring specimens cast from the same mixing batch.

The analytical expressions required to assess the incremental elastic stress developed $\Delta\sigma_{el}$, and the maximum residual stress developed σ_θ (at $r = R_{I,o}$ [39–41]) are noted in [3,35–38]:

$$\Delta\sigma_{el} = -\Delta\varepsilon_{FS}\left[\frac{(1+\upsilon_{inv})R_{I,i}^2 + (1-\upsilon_{inv})R_{I,o}^2}{\left(R_{I,o}^2 - R_{I,i}^2\right)E_{inv}} + \frac{(1-\upsilon_c)R_{I,o}^2 + (1+\upsilon_c)R_{O,i}^2}{\left(R_{O,i}^2 - R_{I,o}^2\right)E_c}\right]^{-1}\frac{R_{I,o}^2 + R_{O,i}^2}{R_{O,i}^2 - R_{I,o}^2} \tag{1}$$

$$\sigma_\theta(r = R_{I,o}) = -\varepsilon_I E_{inv}\left[\frac{R_{O,i}^2 + R_{I,o}^2}{R_{O,i}^2 - R_{I,o}^2}\frac{R_{I,o}^2 - R_{I,i}^2}{2R_{I,o}^2}\right] - \varepsilon_O E_{inv}\left[\frac{R_{O,o}^2 - R_{O,i}^2}{2R_{O,i}^2}\frac{2R_{O,i}^2}{R_{O,i}^2 - R_{I,o}^2}\right] \tag{2}$$

Further details regarding the analytical expressions and their derivation can be found elsewhere [22,36,37,40–42]. The ratio of the residual stress over the elastic stress at any given time yields the stress relaxation ratio σ_R (unitless), i.e.,

$$\sigma_R(t) = \sigma_\theta(t)/\sigma_{el}(t) \tag{3}$$

The stress relaxation ratio indicates the effects of viscoelastic (stress) relaxation as a result of which the residual stress is substantially lower than the elastic stress (i.e., the stress developed following Hooke's law for the ring geometry). It should be noted that the stress relaxation ratio was "zeroed" to 1 day since measurements of free shrinkage were initiated at this time.

3. Results and discussion

3.1. Strength behavior: contrasting the effects of soft and stiff inclusions

Fig. 3(a) shows the measured splitting tensile strength (f_t) for the neat cement paste, and mortars containing PCM and quartz inclusions. Interestingly, all specimens show similar tensile strengths independent of the presence of, and type of inclusions present. This indicates that the splitting tensile strength of the mixtures is "paste controlled". As such, for the inclusions present; i.e., PCM (weaker than the paste matrix), and quartz (stronger than the paste matrix), in both cases the failure of the paste, and hence its tensile strength dictates the failure of the overall composite. Often the splitting tensile strength of cementitious

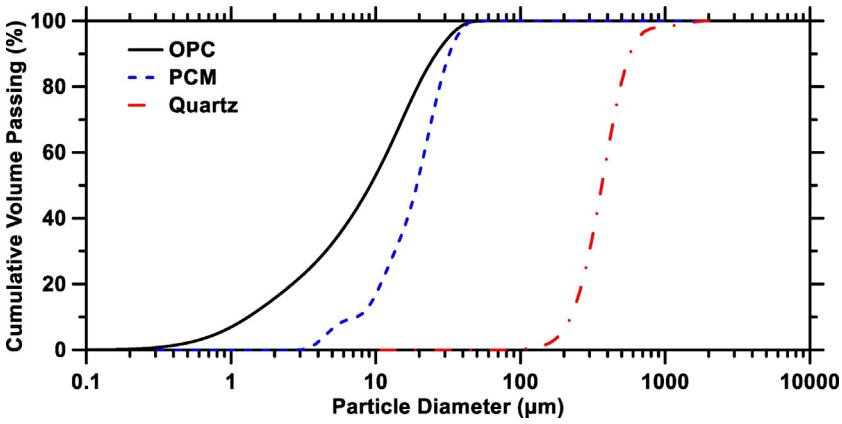

Fig. 2. The particle size distributions of the OPC, quartz, and microencapsulated PCM particulates as measured using static light scattering (SLS).

mixtures is assumed to be on the order of 10% of the compressive strength (f_c), e.g., see Fig. 1(b) [32,43,44]. While this *rule-of-thumb* remains valid for both the neat cement paste, and quartz containing mixtures (e.g., herein, $f_t \approx 0.12f_c$ at an age of 28 days) – it is violated in the case of the PCM-containing mixtures wherein reductions in the compressive strength do not correlate with reductions in the tensile strength. This is an important observation which indicates that: (i) compressive-to-tensile strength correlations should not be applied "as is" to mixtures containing soft inclusions, in general, and, (ii) while in the case of compressive loading PCM inclusions act as a strength-reducing defect in the system – as elaborated below, in the case of tensile loading, their high compliance, and low modulus ensures that only the paste matrix transfers, and resists stresses (albeit for the range of PCM volume fractions considered) – as a result of which the tensile strength of all formulations is similar to that of the neat paste.

It should furthermore be noted that in the case of compressive loading, when the inclusions are stiffer than the paste, assuming near-perfect bond between the inclusions and matrix, stresses concentrate within the inclusions. For this reason, in the case of the quartz inclusions, the compressive strength is similar across all dosages – as failure only occurs when the stress capacity of the paste is exceeded (i.e., since the paste is weaker than the quartz inclusions, see Fig. 1b). On the other hand, when the inclusions are compliant, stresses concentrate at the matrix (paste)-inclusion interface – in increasing proportion as the stiffness contrast between the matrix and inclusions enhances. Therefore, even if the interface regions (often referred to as the interfacial transition zone, ITZ, in cementitious systems [45–47]) are considered to demonstrate similar strengths independent of the type of inclusion present – in the event of compressive loading, PCM inclusions induce strength reductions (see Fig. 1b) on account of a risk of interfacial failure that amplifies with an increase in soft (PCM) inclusion dosage [48,49].

Coming back to the case of tensile loading, irrespective of the inclusion stiffness, failure initiates at the apex of the inclusion followed by progressive debonding (i.e., due to dilatation) along the matrix-inclusion interface. As a result, failure is interface-dominated independent of the nature of inclusions present [50] Therefore, for PCM and quartz inclusions which are assumed to feature similar ITZ properties (i.e., similar to the neat cement paste matrix; see similar strengths of inclusion-containing and inclusion-free mixtures in Fig. 3a) – the measured tensile strength is similar over the entire range of inclusion dosages considered herein (see Fig. 3a) [48]. It should be noted however, that the size of the ITZ surrounding the quartz and PCM inclusions is substantially different, i.e., due to the differences in their sizes; e.g., the quartz inclusions are >10 times larger than the PCM inclusions (see Fig. 2, and [10]). Of course, this reasoning anticipates that all the inclusions, whether PCM or quartz, are similarly dispersed within the paste matrix. Furthermore, even if the ITZ were slightly weaker at some, but not all interfacial locations (i.e., for a given inclusion type, and volume fraction) this would not result in noticeable strength alterations as this would require a percolated series of nearest neighbor inclusions – all of which feature similarly weak(er) interfacial zones.

Even in the case of the failure of neat cement paste, although there is no ITZ formed in absence of inclusions, plain paste formulations are expected to feature initial flaws ranging in size from a few microns to 100 μm (i.e., the size of a large cement particle) [51]. These flaws which control tensile (opening) failure, are expected to produce macroscopic behavior similar to that induced by the weaker nature of the ITZ that forms when inclusions are present. Therefore, upon tensile loading,

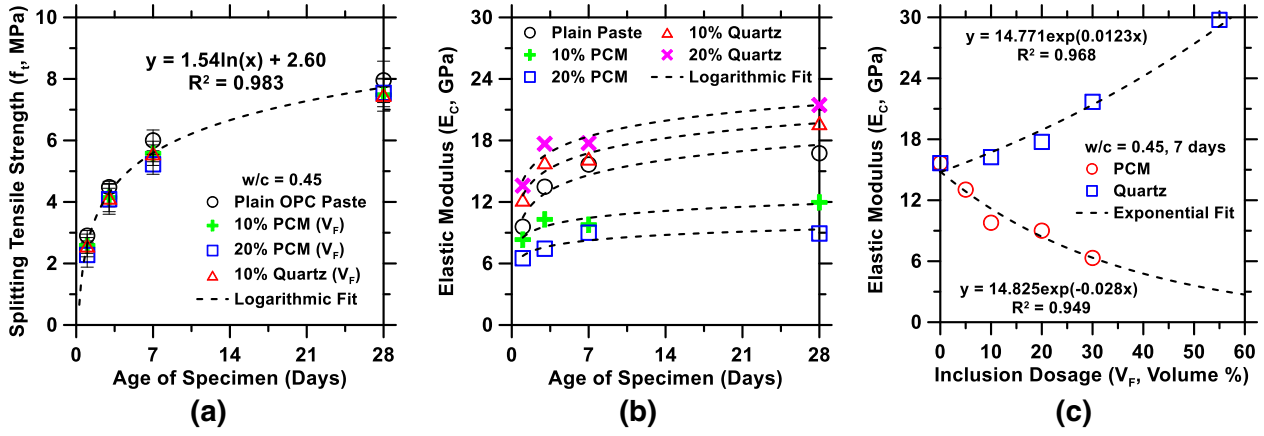

Fig. 3. (a) The splitting tensile strength as a function of specimen age, (b) The static (compressive) elastic modulus as a function of specimen age for the plain cement paste, and quartz and PCM inclusion dosed mixtures, and, (c) The static (compressive) elastic modulus as a function of inclusion dosage after 7 days of curing for quartz and PCM dosed mixtures [10].

whether inclusions are present or not, the cementitious systems shown in Fig. 3(a) show similar tensile resistance (strength). It should be noted however, the cement paste matrix that surrounds PCM inclusions is likely to experience higher tensile stresses at the matrix-inclusion interface as compared to the paste matrix surrounding quartz inclusions – for the same externally applied strain level. This response emanates from the higher compliance of the PCM inclusions as compared to quartz inclusions. However, this effect is not very significant at low inclusion dosages (i.e., ≤20 vol%) in which the inclusions are reasonably well-dispersed, as their interfacial zones, and the stresses that develop therein are not expected to percolate in the microstructure [49].

Figs. 3(b-c) show the compressive elastic modulus E_c of the different cementitious mixtures as a function of time and inclusion dosage. Expectedly, the addition of soft PCM inclusions was found to reduce the elastic modulus, while the dosage of quartz inclusions that are stiffer and stronger than the cement paste increases the elastic modulus [10]. The resulting decrease (PCM) or increase in modulus (quartz) scales as a function of the inclusion dosage in the system – as shown in Fig. 3(c) – and can be reliably estimated using the models of Hobbs [52] and Garboczi and Berryman [53] as shown by Young et al. [54] and Falzone et al. [10]. It should be noted that the data shown in Figs. 3(b-c) is acquired in compression – as such, while the elastic modulus of PCM-containing mixtures is noted to degrade with their increasing dosage, further work is needed to quantify changes in the tensile modulus of such systems, and any changes therein as a function of the stiffness of inclusions present due to complexities including interface debonding (N.B.: For typical cementitious formulations, the tensile and compressive elastic modulus are often within ±30% of each other [55–59]).

3.2. Unrestrained and restrained volume changes: shrinkage and cracking behavior

Fig. 4 shows the shrinkage response of the plain and inclusion-containing cementitious mixtures as a function of time for two drying regimes, i.e., partially sealed over the first 7 days, followed by: (i) drying at 50% RH (Fig. 4a), and, (ii) 75% RH (Fig. 4b) over the subsequent 3 days. Expectedly, both series of mixtures show a similar extent of free shrinkage and mass loss over the first 7 days. After 7 days, expectedly, mixtures exposed to 50% RH lose more mass and shrink at a higher rate than mixtures dried at 75% RH. It is important to note that while both the quartz and PCM mixtures show a similar extent of mass loss (i.e., when normalized by the mass of paste in the system) – in the case of shrinkage, quartz-containing mixtures shrink slightly less than those containing PCM, or the plain paste mixture due to the restraint to paste shrinkage offered by the stiff quartz inclusions [60].

The PCM inclusions on the other hand, due to their compliant nature are unable to restrain the shrinkage of the paste – as a result, the plain and PCM-containing mixtures shrink equivalently; in terms of their rate and extent of shrinkage. Such behavior was also observed by Egan et al. [60] who noted that when the inclusions are impermeable (or less permeable than the cement paste) – moisture loss, but not shrinkage, can be simply described by normalizing the mass loss data by the mass fraction of cement paste in the composite. The shrinkage data shown in Fig. 4 serves as an input into Eq. (1) to calculate the elastic stress developed (and hence infer the extent of stress relaxation [40, 42]) in the PCM and quartz mixtures as a function of time.

Fig. 5(a–b) shows the residual stress developed in the plain paste, and PCM- and quartz-containing specimens as a function of time. Residual stress development over the first 7 days, i.e., when the ring setup is double-bagged to ensure partially sealed conditions – is noted to scale in the order: 10% quartz > neat paste > 10% PCM > 20% PCM. Given that these mixtures all show similar levels of shrinkage over the first 7 days (in fact, the 10% quartz mixture shrinks slightly less than the other compositions; see Fig. 4a) – the scaling in (tensile) residual stresses appears to follow the magnitude of the elastic modulus of these materials; which also scales in the same order (e.g., see Fig. 3c). When the cementitious mixtures are exposed to drying – the rate of stress development increases dramatically until the specimen cracks. It is important to note that the rate of stress development is similar across all mixtures whether drying occurs at 50% RH or 75% RH (see Fig. 5c).

In fact, the stress curves for drying at different RHs trace the same envelope – with cracking occurring at a slightly lower stress level for mixtures dried at 50% RH – as compared to mixtures dried at 75% RH (see also Fig. 6a). Such behavior was also noted by Sant in the case of residual stress development in cement pastes that were exposed to RHs in the range from 50%-to-87% RH [61]. This is because up on exposure to an ambient RH that is lower than the internal RH, cementitious mixtures rapidly lose moisture. The rate of such moisture loss depends upon the diffusion coefficient of moisture within the cement paste (on the order of 10^{-12} m^2/s for a cement paste with w/c = 0.45 [62,63]); as a result a steeper moisture gradient manifests in a material dried at a lower RH, than a material dried at a higher RH [62]. The presence of a steeper moisture and shrinkage gradient would result in a larger level of shrinkage-induced microcracking in the paste dried at 50% RH as compared to that dried at 75% RH. Therefore, due to the faster, and amplified accumulation of damage in the former (see Fig. 5c), and a shorter time interval for stress relaxation (i.e., on account of a faster rate and extent of loading upon drying), formulations dried at 50% RH experience accelerated macroscopic damage localization (cracking) as compared to formulations dried at 75% RH. This suggests that cracking in these

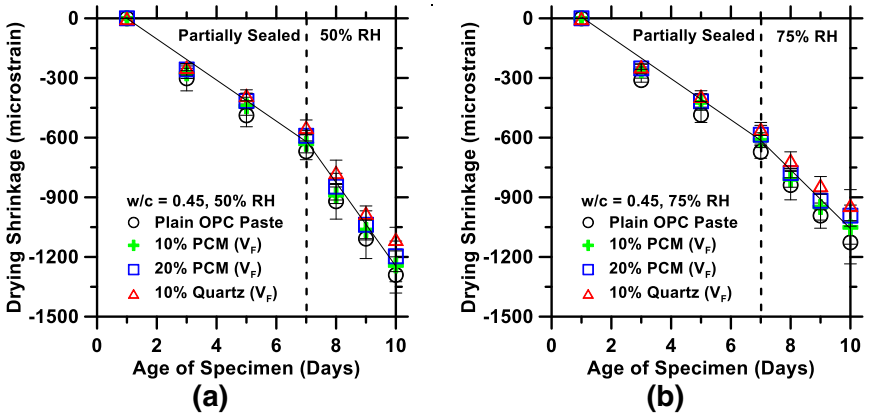

Fig. 4. (a) Free shrinkage as a function of time for plain cement paste, and quartz and PCM inclusion dosed mixtures. The rate of shrinkage in the partially sealed and 50% RH drying periods is on the order of −100 με/day and −200 με/day, respectively. The mass loss from 1-to-7 days, and from 7-to-10 days is on the order of 0.35% and 2.15%, respectively (by mass of cement paste), and, (b) Drying shrinkage as a function of time for plain cement paste, and quartz and PCM inclusion dosed mixtures. The rate of shrinkage in the sealed and 75% RH drying periods is on the order of −100 με/day, and, −145 με/day, respectively. The mass loss from 1-to-7 days, and from 7-to-10 days is on the order of 0.35% and 1.80%, respectively (by mass of cement paste). The solid black lines show the general trend of the dataset.

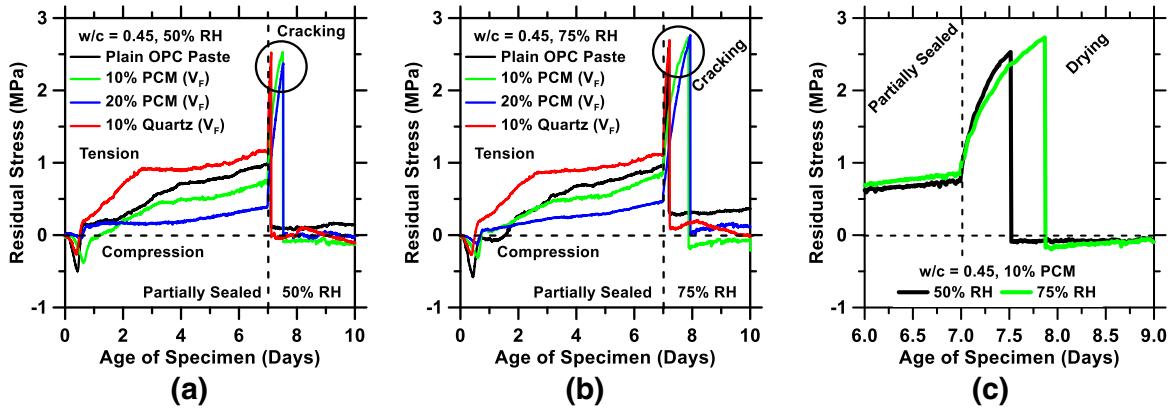

Fig. 5. Residual stress development measured using the dual ring setup as a function of time for plain cement paste, and quartz and PCM inclusion dosed mixtures. After 7 days of partially sealed curing the specimens were dried symmetrically, i.e., from their top and bottom surfaces at: (a) 50% RH, and, (b) 75% RH. The time at which the stress drops sharply indicates macroscopic damage localization (cracking), when a single-crack formed in the ring samples. (c) A comparison of residual stress development in the 10% PCM mixture upon drying at 50% RH and 75% RH. The stress development curves show *near-overlap* with each other. The measured stresses represent the average of duplicate ring specimens.

materials manifests as a fracture (i.e., crack growth) controlled rather than a stress (i.e., strength of materials) controlled circumstance.

Significantly, all specimens including the PCM-containing specimens fail at similar stresses – indicative of their similar strengths (see also Fig. 3a). Nevertheless, it is important to note that all the cementitious mixtures fail at tensile stresses substantially (around 50%) lower than the tensile strength of the material around 7 days (see Fig. 6a). This is postulated to be on the account of the formation and sub-critical growth of microcracks in the ring specimens over the first 7 days at sub-critical stresses (e.g., at 3 days, the residual stress developed is $\leq 0.25 f_t$ across all mixtures). As a result, when the ring specimens are exposed to aggressive drying beyond 7 days, the microcracks (flaws, defects) that are initially present rapidly grow until they coalesce. Thus, the materials fail at stress levels lower than their *pristine* tensile strength {N.B.: in a typical cement paste, the initial flaw/crack size is on the order of 100 μm, i.e., the size of a large cement particle [51]}. Therefore, the failure process is dictated by the evolution of incremental and accumulative damage resulting in the degradation of the tensile capacity of the material as compared to a "pristine" cementitious material that would typically fail only in the vicinity of a major flaw, or at a stress level similar to or greater than its tensile strength (i.e., due to the inherent distribution and variability in the material properties) [64,65].

Coming back to the time of cracking (i.e., from when drying at 50% RH or 75% RH is initiated until the specimen fails), expectedly, the time to cracking is extended when drying is carried out at 75% RH rather than 50% RH; due to the slower rate of damage accumulation, and the extended time period available for stress relaxation. It is furthermore important to note that while all the cementitious formulations fail at similar stresses, PCM-containing cementitious materials show a significantly extended time to cracking (e.g., see Fig. 6b). For example, up on exposure at both 50% RH and 75% RH, and for an inclusion dosage of 10 vol% PCM-containing mixtures demonstrate a $\geq 4.5\times$ increase in the time to cracking as compared to quartz-containing mixtures. Close examination of the stress relaxation ratio shown in Fig. 6(c) reveals that the extent of stress relaxation is broadly similar for the plain cement paste, and mixtures containing 10 vol% of either quartz or microencapsulated PCM inclusions. However, the extent of stresses relaxed is substantially enhanced in the mixture containing 20 vol% PCM. When considered in the context of the time to cracking – this suggests that the addition of PCMs at low dosages ensures benefits associated with crack deflection and blunting (i.e., which increases the crack tortuosity and necessitates a higher driving force for crack propagation), such that in spite of the similar levels of stress relaxation, an increase in time to cracking is observed (see Fig. 6b) [19,20,66]. As the PCM inclusion volume fraction is increased yet further – the improved compliance (enhanced stress relaxation) offered by PCM-containing mixtures superimposes on top of the effects of crack blunting and deflection such that the time to cracking enhances further – although only slightly so as compared to the 10 vol% PCM formulations. It is important to note that other soft inclusions with a compliance similar to that of the PCM microcapsules (e.g., elastomers, expanded polystyrene) are expected to offer similar benefits in cementitious composites, i.e., in terms of

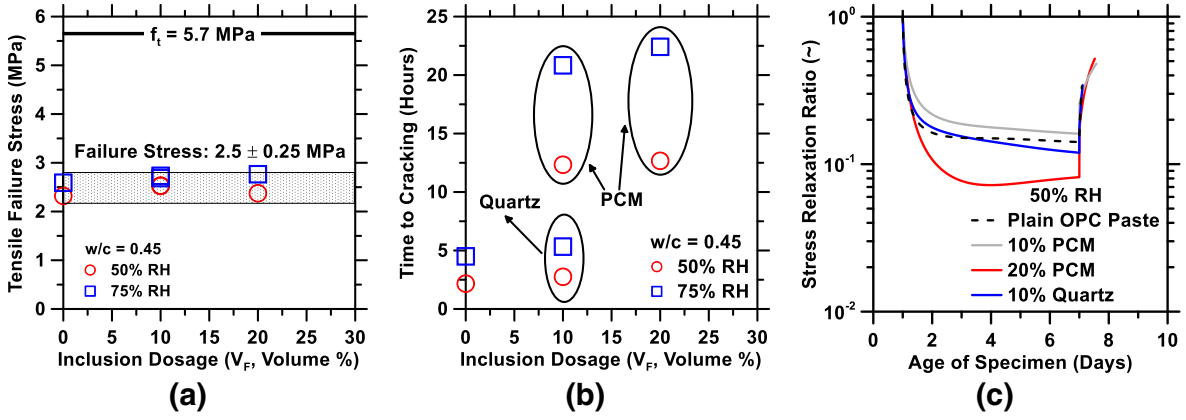

Fig. 6. (a) The stress at failure, and, (b) the time to failure from when drying was initiated at 7 days as a function of the inclusion volume fraction V_F (volume %) for the plain cement paste, and quartz- and PCM-containing specimens. The failure stress and the time to failure represent the average of duplicate ring specimens, and (c) The stress relaxation ratio (σ_R, unitless) calculated for the plain cement paste, and quartz and PCM inclusion dosed mixtures.

increasing the time to cracking [19–21,67]. However, if controlling early- or later-age temperature rise and gradients is specifically desired, the latent heat storage offered by PCM inclusions makes their use mandatory [3–5,17,68].

The beneficial effects of PCM additions were also observed by Fernandes et al. [3] who noted that the critical crack tip opening displacement ($CTOD_c$, in mm) of PCM-containing mixtures, which accounts for interlock effects of the microstructural components, was higher than that of formulations devoid of compliant PCM inclusions. Furthermore, the fracture toughness K_{IC} of PCM-dosed mortars was also found to be similar to or slightly higher than that of neat cement paste; for PCM dosages of ≤20 vol% [3]. Therefore, it appears as though a reduction in material stiffness in the vicinity of a crack (i.e., due to the incorporation of compliant PCM particulates) results in the material being able to undergo larger inelastic deformations in the direction of crack-opening prior to the formation (coalescence) of a macro-crack, as a result of which the $CTOD_c$ increases. Indeed, close examination of the strain energy release rates G_R determined via notched beam fracture tests has indicated that, in the case of PCM containing mixtures, the inelastic component of G_R is dominant – indicating that more energy is being dissipated via inelastic deformations [3]. This increase in inelastic deformations as compared to those of neat (or quartz-containing) cementitious mixtures is thought to induce crack blunting and deflection which enhance the tortuosity of the crack-path; resulting in a heightened resistance to crack propagation [69]. Taken together, these results indicate that the extension in the time to cracking provided by the addition of PCM inclusions is in large part due to the effects of crack blunting and deflection (i.e., which results in a lower rate of microcrack accumulation, coalescence, and propagation), and to a smaller extent on account of an improved ability for stress relaxation (i.e., higher compliance). These results substantiate the premise that the dosage of soft inclusions does not amplify the risk of cracking – rather, dosage of compliant microscale inclusions is noted to valuably enhance the cracking-resistance of cementitious composites.

Furthermore, the outcomes of this work provide critical inputs for modeling the influences of soft inclusions on the cracking behavior of matrix-(soft) inclusion composites as follows. First, it is demonstrated that the often-assumed scaling relation that the tensile strength reduces in fixed proportion with the compressive strength in cementitious composites (e.g., $f_t:f_c \approx 1:10$) [32,43] is invalid when soft inclusions are present. As such, rather than remaining fixed, the ratio $f_t:f_c$ can take values ranging from 1:12 to 1:4.5 as the dosage of soft (PCM) inclusions elevates from 0 vol% to 20 vol%. Second, the coupled effects of viscoelasticity, and crack blunting/deflection on reducing cracking sensitivity are quantified by the stress relaxation ratio (σ_R). In combination, these quantifications of strength scaling relations and extent of stress relaxed provide a means to correctly assess: (a) tensile fracture resistance from a common measurement of compressive strength, and (b), how soft inclusions may affect cracking behavior beyond the effects of softening (i.e., stiffness reduction) by crack blunting and deflection actions; these variables are relevant for enabling precise calculations of crack sensitivity.

4. Summary and conclusions

By carefully combining measurements of tensile strength, and restrained and unrestrained shrinkage, this paper has comprehensively examined the influences of compliant, microscale PCM inclusions on the cracking resistance of cementitious composites. Significantly, it is noted that in spite of inducing substantial reductions in the compressive strength of cementitious composites, the dosage of PCM inclusions induces no change in the tensile capacity (strength) of the material; compared with neat cementitious mixtures, or those containing inclusions stiffer than the paste matrix. This is because tensile failure is an interface-controlled process – which being similar across all formulations, for the volume fractions considered – ensures that the tensile strength remains unchanged and independent of the type of inclusions present. Furthermore, PCM-containing specimens show a substantial delay in their time to cracking (e.g., by ≥4.5× for the inclusion dosages considered) as compared to neat, or quartz-containing cementitious mixtures. Such extensions in the time to cracking were attributed dominantly to the effects of crack-blunting and deflection induced by the PCM inclusions; and to a lesser extent to enhanced stress relaxation. Taken together, these results indicate that in contrast to the (intuitive) expectation of an amplified cracking risk – the addition of compliant, microscale PCM (and other soft) inclusions in fact reduces the risk of and time to cracking in cementitious composites.

Acknowledgements

The authors acknowledge financial support for this research provisioned by: Infravation ERA-NET grant (ECLIPS: 31109806.0001), Department of Energy (DE-NE0008398), National Science Foundation (CMMI: 1130028, CAREER: 1253269) and the California Energy Commission (CEC Contract: PIR: 12-032). The authors also acknowledge discretionary financial support provided by the Office of the Vice-Chancellor for Research at UCLA via the 'Sustainable L.A. Grand Challenge'. The contents of this paper reflect the views and opinions of the authors who are responsible for the accuracy of data presented. This research was carried out in the Laboratory for the Chemistry of Construction Materials (LC^2) and Molecular Instrumentation Center at UCLA. As such, the authors gratefully acknowledge the support that has made these laboratories and their operations possible.

References

[1] F. Kuznik, D. David, K. Johannes, J.-J. Roux, A review on phase change materials integrated in building walls, Renew. Sust. Energ. Rev. 15 (2011) 379–391.
[2] J. Chen, F.J. Liu, Y.F. Zheng, Review on phase change material slurries, Adv. Mater. Res. 860 (2014) 946–951.
[3] F. Fernandes, S. Manari, M. Aguayo, K. Santos, T. Oey, Z. Wei, G. Falzone, N. Neithalath, G. Sant, On the feasibility of using phase change materials (PCMs) to mitigate thermal cracking in cementitious materials, Cem. Concr. Compos. 51 (2014) 14–26.
[4] D.P. Bentz, R. Turpin, Potential applications of phase change materials in concrete technology, Cem. Concr. Compos. 29 (2007) 527–532.
[5] A.M. Thiele, Z. Wei, G. Falzone, B.A. Young, N. Neithalath, G. Sant, L. Pilon, Figure of merit for the thermal performance of cementitious composites containing phase change materials, Cem. Concr. Compos. 65 (2016) 214–226.
[6] C.M. Lai, S. Hokoi, Thermal performance of an aluminum honeycomb wallboard incorporating microencapsulated PCM, Energy Build. 73 (2014) 37–47.
[7] N. Soares, J.J. Costa, A.R. Gaspar, P. Santos, Review of passive PCM latent heat thermal energy storage systems towards buildings' energy efficiency, Energy Build. 59 (2013) 82–103.
[8] S. Ogden, L. Klintberg, G. Thornell, K. Hjort, R. Boden, Review on miniaturized paraffin phase change actuators, valves, and pumps, Microfluid. Nanofluid. 17 (2014) 53–71.
[9] Z. Wei, F. Galzone, B. Wang, A. Thiele, G. Puerta-Falla, L. Pilon, N. Neithalath, G. Sant, The durability of cementitious composites containing microencapsulated phase change materials, Cement Concr. Compos. 81 (2017) 66–76.
[10] G. Falzone, G. Puerta, Z. Wei, M. Zhao, A. Kumar, M. Bauchy, N. Neithalath, L. Pilon, G. Sant, The influences of soft and stiff inclusions on the mechanical properties of cementitious composites, Cem. Concr. Compos. 71 (2016) 153–165.
[11] M. Hossain, C. Ketata, Experimental study of physical and mechanical properties of natural and synthetic waxes using uniaxial compressive strength test, Proceeding of Third International Conference on Modeling, Simulations and Applied Optimalization 2009, pp. 1–5.
[12] M.S. Stetsenko, Determining the elastic constants of hydrocarbons of heavy oil products using molecular dynamics simulation approach, J. Pet. Sci. Eng. 126 (2015) 124–130.
[13] Y. Miyazaki, A.G. Marangoni, Structural-mechanical model of wax crystal networks -a mesoscale cellular solid approach, Mater. Res. Expr. 1 (2014) 1–12.
[14] J. Giro-Paloma, G. Oncins, C. Barreneche, M. Martinez, A.I. Fernandez, L.F. Cabeza, Physico-chemical and mechanical properties of microencapsulated phase change material, Appl. Energy 109 (2013) 441–448.
[15] J.F. Su, X.Y. Wang, H. Dong, Micromechanical properties of melamine-formaldehyde microcapsules by nanoindentation: effect of size and shell thickness, Mater. Lett. 89 (2012) 1–4.
[16] M.T. Hosamani, N.H. Ayachit, D.K. Deshpande, On the viscoelastic and dielectric behavior of some organic compounds and their binary mixtures, J. Macromol. Sci. B Phys. 48 (2009) 550–561.
[17] B.A. Young, Z. Wei, J. Rubalcava-Cruz, G. Falzone, A. Kumar, N. Neithalath, G. Sant, L. Pilon, A general method for retrieving thermal deformation properties of

microencapsulated phase change materials or other particulate inclusions in cementitious composites, Mater. Des. 126 (2017) 259–267.
[18] M. Hunger, A.G. Entrop, I. Mandilaras, H.J.H. Brouwers, M. Founti, The behavior of self-compacting concrete containing micro-encapsulated phase change materials, Cem. Concr. Compos. 31 (2009) 731–743.
[19] K.C. Jajam, H.V. Tippur, Role of inclusion stiffness and interfacial strength on dynamic matrix crack growth: an experimental study, Int. J. Solids Struct. 49 (2012) 1127–1146.
[20] J. Tirosh, W. Nachlis, D. Hunston, Strength behavior of toughened polymers by fibrous (or particulate) elastomers, Mech. Mater. 19 (1995) 329–342.
[21] M. Trussoni, C.D. Hays, R.F. Zollo, Fracture properties of concrete containing expanded polystyrene aggregate replacement, ACI Mater. J. 110 (2013) 549–558.
[22] K.J. Shin, B. Bucher, J. Weiss, Role of lightweight synthetic particles on the restrained shrinkage cracking behavior of mortar, J. Mater. Civ. Eng. 23 (2011) 597–605.
[23] A. Schwartzentruber, M. Philippe, G. Marchese, Effect of PVA, glass and metallic fibers, and of an expansive admixture on the cracking tendency of ultrahigh strength mortar, Cem. Concr. Compos. 26 (2004) 573–580.
[24] A. Turatsinze, J.L. Granju, S. Bonnet, Positive synergy between steel-fibres and rubber aggregates: effect on the resistance of cement-based mortars to shrinkage cracking, Cem. Concr. Res. 36 (2006) 1692–1697.
[25] ASTM International, ASTM Standard C305: Standard Practice for Mechanical Mixing of Hydraulic Cement Pastes and Mortars of Plastic Consistency, West Conshohocken, PA, 2014.
[26] ASTM International, ASTM Standard C778: Standard Specification for Standard Sand, West Conshohocken, PA, 2013.
[27] Microtek Laboratories, Inc., http://www.microteklabs.com/data-sheets.html (Accessed February 5, 2017).
[28] C.F. Ferraris, V.A. Hackley, A.I. Avilés, Measurement of particle size distribution in portland cement powder: analysis of ASTM round robin studies, Cem. Concr. Aggregate 26 (2004) 1–11.
[29] G. Gao, S. Moya, H. Lichtenfeld, A. Casoli, H. Fiedler, E. Donath, H. Moehwald, The decomposition process of melamine formaldehyde cores: the key step in the fabrication of ultrathin polyelectrolyte multilayer capsules, Macromol. Mater. Eng. 286 (2001) 355–361.
[30] G. Ghosh, Dispersion-equation coefficients for the refractive index and birefringence of calcite and quartz crystals, Opt. Commun. 163 (1999) 95–102.
[31] ASTM International, ASTM Standard C496/C496M: Standard Test Method for Splitting Tensile Strength of Cylindrical Concrete Specimens, West Conshohocken, PA, 2011.
[32] P.K. Mehta, P.J.M. Monteiro, Concrete: Microstructure, Properties, and Materials, Fourth edition McGraw-Hill, New York, 2014.
[33] ASTM International, ASTM Standard C469/C469M: Standard Test Method for Static Modulus of Elasticity and Poisson's Ratio of Concrete in Compression, West Conshohocken, PA, 2014.
[34] ASTM International, ASTM Standard C157: Standard Test Method for Length Change of Hardened Hydraulic-cement Mortar and Concrete, West Conshohocken, PA, 2014.
[35] H.R. Shah, J. Weiss, Quantifying shrinkage cracking in fiber reinforced concrete using the ring test, Mater. Struct. 39 (2006) 887–899.
[36] J.H. Moon, J. Weiss, Estimating residual stress in the restrained ring test under circumferential drying, Cem. Concr. Compos. 28 (2006) 486–496.
[37] J. Weiss, P. Lura, F. Rajabipour, G. Sant, Performance of shrinkage-reducing admixtures at different humidities and at early ages, ACI Mater. J. 105 (2008) 478–486.
[38] G. Sant, Examining Volume Changes, Stress Development and Cracking in Cement Based Systems(MS Thesis) Purdue University, 2007.
[39] S.P. Timoshenko, J.N. Goodier, Theory of Elasticity, Third edition McGraw-Hill, New York, 1970.
[40] A.B. Hossain, J. Weiss, Assessing residual stress development and stress relaxation in restrained concrete ring specimens, Cem. Concr. Compos. 26 (2004) 531–540.
[41] A.B. Hossain, J. Weiss, The role of specimen geometry and boundary conditions on stress development and cracking in the restrained ring test, Cem. Concr. Res. 36 (2006) 189–199.
[42] G. Sant, The influence of temperature on autogenous volume changes in cementitious materials containing shrinkage reducing admixtures, Cem. Concr. Compos. 34 (2012) 855–865.
[43] ACI, Standard 318: Building Code Requirements for Structural Concrete, Farmington Hills, MI, 2014.
[44] S. Mindess, J.F. Young, D. Darwin, Concrete, Second edition Prentice Hall, New Jersey, 2003.
[45] K.L. Scrivener, A.K. Crumbie, P. Laugesen, The interfacial transition zone (ITZ) between cement paste and aggregate in concrete, Interf. Sci. 12 (2004) 411–421.
[46] R. Gao, P. Stroeven, Particle packing and microstructure of the ITZ in cement-based materials, Mcci'2000: International Symposium on Modern Concrete Composites & Infrastructures, Vol. I, 2000, pp. 105–110.
[47] J. Hu, P. Stroeven, Properties of the interfacial transition zone in model concrete, Interf. Sci. 12 (2004) 389–397.
[48] S. Das, A. Maroli, N. Neithalath, Finite element-based micromechanical modeling of the influence of phase properties on the elastic response of cementitious mortars, Constr. Build. Mater. 127 (2016) 153–166.
[49] M. Aguayo, S. Das, A. Maroli, N. Kabay, J.C.E. Mertens, S.D. Rajan, G. Sant, N. Chawla, N. Neithalath, The influence of microencapsulated phase change material (PCM) characteristics on the microstructure and strength of cementitious composites: experiments and finite element simulations, Cem. Concr. Compos. 73 (2016) 29–41.
[50] V. Birman, K. Chandrashekhara, M.S. Hopkins, J.S. Volz, Strength analysis of particulate polymers, Compos. B Eng. 54 (2013) 278–288.
[51] P. Lura, O.M. Jensen, J. Weiss, Cracking in cement paste induced by autogenous shrinkage, Mater. Struct. 42 (2009) 1089–1099.
[52] D.W. Hobbs, The dependence of the bulk modulus, Young's modulus, creep, shrinkage, and thermal expansion of concrete upon aggregate volume concentration, Mater. Struct. 4 (1971) 107–114.
[53] E.J. Garboczi, J.G. Berryman, Elastic moduli of a material containing composite inclusions: effective medium theory and finite element computations, Mech. Mater. 33 (2001) 455–470.
[54] B.A. Young, A.M.K. Fujii, A.M. Thiele, A. Kumar, G. Sant, E. Taciroglu, L. Pilon, Effective elastic moduli of core-shell-matrix composites, Mech. Mater. 92 (2016) 94–106.
[55] I. Yoshitake, F. Rajabipour, Y. Mimura, A. Scanlon, A prediction method of tensile Young's modulus of concrete at early age, Adv. Civil Eng. 2012 (2012) 1–10.
[56] N.X. Xie, W. Liu, Determining tensile properties of mass concrete by direct tensile test, ACI Mater. J. 86 (1989) 214–219.
[57] S. Swaddiwudhipong, H.R. Lu, T.H. Wee, Direct tension test and tensile strain capacity of concrete at early age, Cem. Concr. Res. 33 (2003) 2077–2084.
[58] I. Yoshitake, W.B. Zhang, Y. Mimura, T. Saito, Uniaxial tensile strength and tensile Young's modulus of fly-ash concrete at early age, Constr. Build. Mater. 40 (2013) 514–521.
[59] I. Yoshitake, H. Komure, A.Y. Nassif, S. Fukumoto, Tensile properties of high volume fly-ash (HVFA) concrete with limestone aggregate, Constr. Build. Mater. 49 (2013) 101–109.
[60] G. Egan, A. Kumar, N. Neithalath, G. Sant, Re-examining the influence of the inclusion characteristics on the drying shrinkage of cementitious composites, Constr. Build. Mater. 146 (2017) 713–722.
[61] G. Sant, Restrained shrinkage cracking in cementitious materials: the role of the external relative humidity and shrinkage reducing admixtures (In Development).
[62] N. Neithalath, Analysis of moisture transport in mortars and concrete using sorption-diffusion approach, ACI J. 103 (2006) 209–217.
[63] K. Sakata, A study on moisture diffusion in drying and drying shrinkage of concrete, Cem. Concr. Res. 13 (1983) 216–224.
[64] A. Radlinska, B. Pease, J. Weiss, A preliminary numerical investigation on the influence of material variability in the early-age cracking behavior of restrained concrete, Mater. Struct. 40 (2007) 375–386.
[65] A. Radlinska, J. Weiss, Toward the development of a performance-related specification for concrete shrinkage, J. Mater. Civ. Eng. 24 (2012) 64–71.
[66] D. Leguillon, C. Lacroix, E. Martin, Matrix crack deflection at an interface between a stiff matrix and a soft inclusion, Damage, Fatigue, Fracture 328 (2000) 19–24.
[67] E.M. Wouterson, F.Y.C. Boey, X. Hu, S.-C. Wong, Specific properties and fracture toughness of syntactic foam: effect of foam microstructures, Compos. Sci. Technol. 65 (2005) 1840–1850.
[68] B.A. Young, G. Falzone, Z. She, A.M. Thiele, Z. Wei, N. Neithalath, G. Sant, L. Pilon, Early-age temperature evolution in concrete pavements containing microencapsulated phase change materials, Constr. Build. Mater. 147 (2017) 466–477.
[69] M. Aguayo, S. Das, A. Maroli, N. Kabay, B. Mobasher, G. Sant, N. Neithalath, Elucidating the influences of compliant microscale inclusions on fracture behavior of cementitious mortars, Int. J. Fract. (Under Review).